1 Part failure prediction in AM

Originally titled "A Strength Tensor Based Failure Criterion with Stress Interactions", it will be referred in this work as the Stress-Stress Interaction Criterion (SSIC). This chapter will briefly describe the Gol'denblat-Kopnov model upon which the SSIC is based, followed by a proper description of how it implements stress interactions. Finally, it will go detail how it was used to develop a failure envelopes for parts produced through AM techniques, focusing on a recent example deployed for FFF parts produced with ABS.

1.1   The Gol'denblat-Kopnov Model

The Gol'denblat-Kopnov Criterion (GKC) describes a mathematical function that depends on the stress state of an anisotropic material. Should the computation of this expression exceed a threshold, part failure is to be expected. To that end, a scalar function that depends on stress tensors that completely characterize the state of the material was developed [**Goldenblat1965**]. This function is shown in Equation **??**, where stresses are denoted σ, and the subindices i,j,k,l denote a particular load direction.

$$f = (F_{ij}\sigma_{ij})^{\alpha} + (F_{ijkl}\sigma_{ij}\sigma_{kl})^{\beta} + (F_{ijklmn}\sigma_{ij}\sigma_{kl}\sigma_{mn})^{\gamma} + ... \qquad (1.1)$$

The terms F_{ij}, F_{ijkl} and F_{ijklmn} represent second, fourth and sixth order tensors respectively. These terms of the equation depend on engineering strength parameters, such as the ultimate tensile and compressive strengths of the material in a particular load direction [**Osswald2017a**]. Due to the complexity associated with using higher order tensors, Gol'denblat and Kopnov limited their approach to using only the second and fourth order terms. Thus Equation **??** is reduced to:

$$f = (F_{ij}\sigma_{ij})^{\alpha} + (F_{ijkl}\sigma_{ij}\sigma_{kl})^{\beta} \qquad (1.2)$$

In order to attain a linear criterion scalar function, the exponents α and β were assigned values of 1 and 1/2 respectively. Finally, in plane stress scenarios, the GKC becomes:

$$f = F_{11}\sigma_{11} + F_{22}\sigma_{22} + F_{12}\tau_{12} + (F_{1111}\sigma_{11}^2 + F_{2222}\sigma_{22}^2 + F_{1212}\tau_{12}^2$$
$$+ 2F_{1122}\sigma_{11}\sigma_{22} + 2F_{1112}\sigma_{11}\tau_{12} + 2F_{2212}\sigma_{22}\tau_{12})^{1/2} \tag{1.3}$$

Note that in Equation ?? σ and τ denote normal and shear stresses respectively. Figure ?? depicts an anisotropic material and all the possible loading directions for reference.

Figure 1.1: Different load directions in an anisotropic material

Per Gol'denblat and Kopnov's design, should the computation of f in Equation ?? be greater or equal to 1, part failure is to be expected. However, to simplify calculations, they deliberately assumed the interaction terms F_{1112} and F_{2212} to be zero. This is an important consideration that will come into play when describing the SSIC.

Most of the terms in the GKC are obtained through mechanical testing of coupons under pure uniaxial loads in the 1 or 2 direction, or pure shear in the 1-2 plane [Osswald2017a]. In these scenarios, f will be equal to 1 at failure, and the stress state will be known to the user, allowing some of the unknown tensorial parameters to be easily calculated. Using F_{11} and F_{1111} as examples, the process would be as follows:

1. The tensile and compressive strength in the 1-1 direction would be obtained through mechanical testing. These values are named X_t and X_c respectively.

2. Under these failure conditions, Equation **??** is reduced to the following system of equations:
$$\begin{cases} 1 = F_{11}X_t + (F_{1111}X_t^2)^{1/2} \\ 1 = -F_{11}X_c + (F_{1111}X_c^2)^{1/2} \end{cases}$$

3. F_{11} and F_{1111} can be obtained, yielding $F_{11} = \frac{1}{2}(\frac{1}{X_t} - \frac{1}{X_c})$ and $F_{1111} = \frac{1}{4}(\frac{1}{X_t} + \frac{1}{X_c})^2$.

The only exception to this procedure would be the F_{1122} component, which requires measuring the positive and negative shear strengths of a coupon with reinforcement oriented in 45°. These parameters are named S_{45p} and S_{45n} respectively. Table **??** summarizes the nomenclature used for the strength parameters required to completely populate the failure function of the GKC. Table **??** summarizes all the tensorial component calculations.

Table 1.1: Nomenclature of the GKC parameters

Parameter	Description
X_t	Tensile strength in the 1-1 direction
X_c	Compressive strength in the 1-1 direction
Y_t	Tensile strength in the 2-2 direction
Y_c	Compressive strength in the 2-2 direction
S_{45p}	Positive shear strength for 45° specimen
S_{45n}	Negative shear strength for 45° specimen
S	Shear strength in the 1-2 plane

Table 1.2: Tensorial components of the GKC

Component	Formula
F_{11}	$\frac{1}{2}(\frac{1}{X_t} - \frac{1}{X_c})$
F_{1111}	$\frac{1}{4}(\frac{1}{X_t} + \frac{1}{X_c})^2$
F_{22}	$\frac{1}{2}(\frac{1}{Y_t} - \frac{1}{Y_c})$
F_{2222}	$\frac{1}{4}(\frac{1}{Y_t} + \frac{1}{Y_c})^2$
F_{12}	0
F_{1212}	$\frac{1}{S^2}$
F_{1122}	$\frac{1}{8}[(\frac{1}{X_t} + \frac{1}{X_c})^2 + (\frac{1}{Y_t} + \frac{1}{Y_c})^2 - (\frac{1}{S_{45p}} + \frac{1}{S_{45n}})^2]$

1.2   The Stress-Stress Interaction Criterion

One of the assumptions made in the GKC is that the components F_{1112} and F_{2212} in Equation **??** are null. While this simplifies the model, it essentially neglects any interactions between axial loads and shear stresses, namely, the σ_{11} - τ_{12} and σ_{22} - τ_{12} interactions. Practically, this causes the failure surface developed through the GKC to under-predict shear strengthening effects exhibited by anisotropic materials loaded in combined axial and shear conditions. The Stress-Stress Interaction Criterion (SSIC) attempts to overcome these limitations by building upon the GKC. For the SSIC, the interaction effects are captured through the use of the slopes of the failure surface at any of the points where the engineering strength is known within a particular stress plane [**Osswald2017a**]. In this failure scenario, the stress state of the coupon is known and easy to implement into Equation **??**, where $f = 1$. The resulting expression can then be derived with respect to one of the stresses, allowing for the interaction components to be calculated. This is better illustrated through an example. Assuming the component of interest is F_{2212}, the procedure to calculate it through the SSIC would be as follows:

1. Obtain all the tensorial components possible through the GKC.

2. Using the σ_{22}–τ_{12} stress plane, take the derivative of Equation **??** as a function of σ_{22} in the scenario of failure under pure shear ($f = 1$). This yields the expression:

$$0 = F_{22} + [F_{1212}S(\frac{d\tau_{12}}{d\sigma_{22}}) + F_{2212}S] \tag{1.4}$$

   where $\frac{d\tau_{12}}{d\sigma_{22}}$ is the slope of the graph at failure under shear. This term is named μ^{2212} in the SSIC and can be obtained by performing combined loading tests.

3. Rearranging Equation **??** to solve for the unknown F_{2212} gives the following expression:

$$F_{2212} = -\frac{F_{22}}{S} - F_{1212}\mu^{2212} \tag{1.5}$$

   A similar procedure can be followed for any σ_{ii}-τ_{ij} interaction, or even any σ_{ii}-σ_{jj} components. For this last scenario, the user has four potential choices of slopes to determine the tensorial component of interest. In the SSIC, any slope obtained from a σ_{ii}-σ_{jj} stress plane is named λ^{iijj}, as opposed to μ^{iiij} for slopes in a σ_{ii}-τ_{ij} reference. A schematic of all possible interaction slopes is shown in Figure **??**, while Table **??** summarizes all the possible interaction factors available through the SSIC, where τ_{ij}^u denotes ultimate shear strength in a particular shear plane.

Figure 1.2: Interaction slopes available through the SSIC

Table 1.3: Interaction components attainable through the SSIC [**Osswald2017a**]

Component	Formula
F_{iiij}	$-\frac{F_{ii}}{\tau_{ij}^u} - F_{ijij}\mu^{iiij}$
F_{iijj} through λ_1^{iijj}	$-\frac{(F_{ii}+F_{jj}\lambda_1^{iijj})F_{iiii}^{1/2}+F_{iiii}}{\lambda_1^{iijj}}$
F_{iijj} through λ_2^{iijj}	$-(F_{ii}+F_{jj}\lambda_2^{iijj})F_{jjjj}^{1/2} - F_{jjjj}\lambda_2^{iijj}$
F_{iijj} through λ_3^{iijj}	$\frac{(F_{ii}+F_{jj}\lambda_3^{iijj})F_{iiii}^{1/2}-F_{iiii}}{\lambda_3^{iijj}}$
F_{iijj} through λ_4^{iijj}	$(F_{ii}+F_{jj}\lambda_4^{iijj})F_{jjjj}^{1/2} - F_{jjjj}\lambda_4^{iijj}$

1.2.1 Applications of the SSIC in AM

The SSIC offers a way of capturing in a more accurate manner the different failure modes of parts produced through AM technologies. As an example, the model has been successfully implemented by Obst *et al.* in 2018 for SLS manufactured parts produced with PA12 [**Obst2018**, **Obst2017**]. Their results show how the model was able to capture the τ_{12}-σ_{22} and σ_{11}-σ_{22} interactions. The failure surface obtained, shown in Figure **??**, was able to capture the interactions between certain axial and transverse stresses. However, due to the limitations of the SLS process, it was not possible to measure the interaction slope between the τ_{12} and σ_{11} directions.

Figure 1.3: Failure surface for SLS developed through the SSIC [**Obst2018**]

Recent unpublished work by Osswald *et al.* [**Osswald2020**] generated a failure envelope for Multi-Jet Fusion (MJF) parts produced using PA12, and compared it to the surface obtained by Obst *et al.* [**Obst2018**]. Results indicate that, while both techniques are based on Powder Based Fusion (PBF) and use the same material, the envelopes for each AM technology were distinct, serving as proof that these technologies are not as comparable under complex loading conditions as previously assumed. The transverse-axial interaction for the MJF case was significantly less pronounced than for SLS, further reinforcing that each AM technique needs to be studied in a case-by-case basis in terms of mechanical failure characterization.

In 2019, Mazzei Capote *et al.* [**MazzeiCapote2019**] developed a failure envelope for FFF parts produced using a customized ABS filament produced in-house. Specimens were produced using either a commercially available desktop FFF printer

Figure 1.4: Comparison of the $\sigma_{22} - \tau_{12}$ interaction for SLS and MJF PA12 parts [**Osswald2020**]

(Lulzbot TAZ5, USA), or a customized 6-axis robotic printing solution whenever the bead orientation was hard to achieve using a *2.5-D* machine. The robotic printer was based on a 6-axis robot (ABB IRB-120, Switzerland) and fitted with a stationary printhead mounted on an aluminum frame, chosen to be the same extruder from the traditional printer (LulzBot TAZ Single Extruder Tool Head v2, 0.5 mm nozzle, USA) to minimize machine influence on the results [**VanHulle2017**]. The final surface obtained showed significant stress interactions in certain directions. Starting with the σ_{11}-σ_{22} plane, it can be seen that the failure envelope has a slight tilt. Refer to Figure **??** for a graph showing the calculated failure envelope, including the experimental data for reference. This tilt is evidence of an interaction between the transverse and longitudinal stresses. The conclusion is that FFF parts produced with the print parameters used in the study should show strengthening when loaded bi-axially in compression.

Figure 1.5: σ_{11}-σ_{22} plane including data for reference.

Using the results from combined loading tests plotted in the $11 - 12$ and $22 - 12$ planes allows visualization of the transverse-axial stress interactions. Beginning with the $11 - 12$ plane, it can be seen that the calculated interaction slope μ^{1112} equals 5.2×10^{-3}, a value that's practically zero. Using this parameter, the failure surface shown in Figure **??** can be obtained. A dashed line representing μ^{1112} is added for reference. The $22-12$ plane by comparison reveals a considerable slope. It can be seen through the use of combined loads that there is a slight decrease in the shear strength of the specimens when a tensile load is applied in the $2 - 2$ direction. A slope of -0.2 was obtained for μ^{2212}. Figure **??** shows the resulting surface with the data and a line with a slope of -0.2 overlaid for reference.

Figure 1.6: σ_{11}-τ_{12} plane including data for reference.

Figure 1.7: σ_{22}-τ_{12} plane including data for reference.

The use of this envelope to predict part failure was tested by Mazzei Capote [**MazzeiJCompSci**] *et al.* in 2019. In this study, the failure function was used to estimate the failure stress of mechanical coupons loaded under tension, with a variety of raster angles being used to generate a complex loading state in the local coordinate system. Results indicated the failure prediction boundary was within 5 to 10% of the

real value. Results are summarized in Figure **??**, where the average of 5 mechanical tests per raster angle is represented in a dot, and the SSIC predicted failure stress is shown in a bright red line. These are compared to simpler FC, such as the maximum stress criteria in the σ_{11}, σ_{22}, and τ_{12} directions, labeled M1-1, M2-2, and M1-2 respectively.

(a) Loading
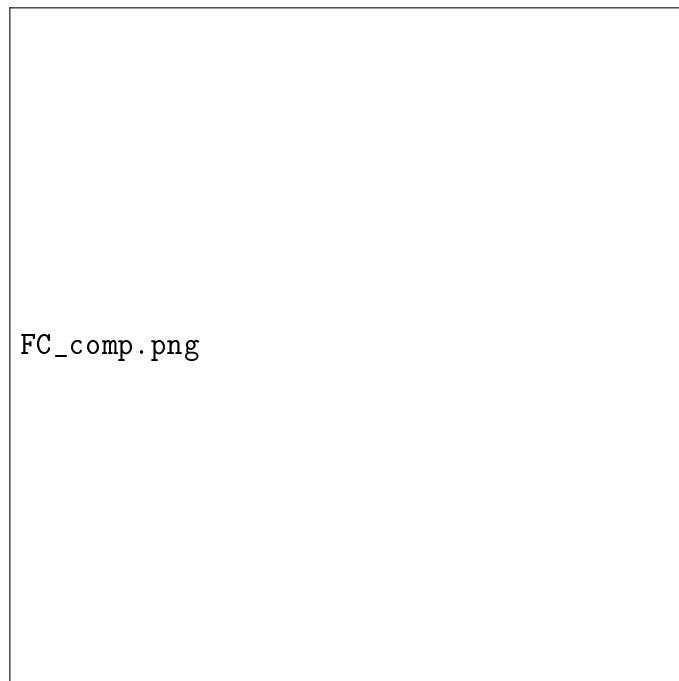
(b) Comparison of data and failure prediction using various
FC

Figure 1.8: Results from [**MazzeiJCompSci**]

While the use of FC in AM is promising, its adoption has been limited in scope. Part of the problem lies in the large number of mechanical tests required to achieve a trustworthy failure envelope, as well as the requirement of specialized equipment – such as a variety of mechanical testing devices, as well as specialized printing solutions as seen in the FFF failure envelope. Chapter **??** outlines proposed work aimed at predicting the mechanical response of FFF parts using machine learning methods. Some, if not all of the concepts explored could easily be extrapolated to other AM techniques. It should be noted that the two methods are not mutually exclusive. A combination of both FC and machine learning predictive methods can hopefully lead to a higher adoption rates of AM in industrial scenarios where the final desired application involves complex mechanical loads upon the finished part.